RESEARCH

Evaluation of spatial and temporal dynamics of seawater intrusion in coastal aquifers of southeast India: insights from hydrochemical facies analysis

Prabhakaran Moorthy · Sridhar Sundaramoorthy · Priyadarsi D. Roy · Tune Usha · Sisir Kumar Dash · Muthusankar Gowrappan · Lakshumanan Chokklingam

Abstract This study aims to investigate and understand the temporal and spatial movement of seawater intrusion into the coastal aquifers. Groundwater salinity increase has affected the entire eastern part of the study area and is primarily influenced by direct and reverse ion exchange reactions associated with intrusion and freshwater influx phases, which alternate over monsoons. To gain insights into the spatiotemporal dynamics of the seawater intrusion process, hydrochemical facies analysis utilizing the HFE-Diagram was employed. Additionally, the study considered the major ionic changes during both the monsoons. The HFE-Diagram analysis of hydrochemical facies revealed distinctions in the behaviour of each coastal aquifer concerning seawater intrusion-induced salinization. In PRM 2020, the data shows that approximately 65% of the samples fall under the freshening phase, while the remaining 35% were categorized as intrusion phase. Within the freshening phase, seven different hydrochemical facies were identified, including Na-Cl, Na-MixCl, MixNa-MixCl, Na-MixHCO$_3$/MixSO$_4$, MixNa-MixSO$_4$, Na-HCO$_3$, and MixCa-HCO$_3$. In contrast, the intrusion phase had four facies: MixCaMixHCO$_3$, MixNa-Cl, Ca-Cl, and Na-Cl. Especially, the Na-Cl facies (f$_1$) within the freshening phase attributed for the largest percentage, contributing 30% of the samples. In POM 2021, the distribution of samples shifted slightly, with approximately 72.5% belonging to the freshening phase and 27.5% to the intrusion phase. Within the freshening phase of POM 2021, five hydrochemical facies were identified: Na-Cl, Na-MixCl, Na-MixHCO$_3$/MixSO$_4$, MixNa-MixSO$_4$, and Na-HCO$_3$. The intrusion phase of POM 2021 had three facies: MixNa-Cl, Na-Cl, and MixCa-Cl. Similar to PRM 2020, the Na-Cl facies (f$_1$) remained the most predominant in the freshening phase, comprising 30% of the samples. The relation between total dissolved solids (TDS) and various ionic ratios, such as HCO$_3^-$/Cl$^-$, Na$^+$/Cl$^-$, Ca^{2+}/Cl$^-$, Mg^{2+}/Cl$^-$, K$^+$/Cl$^-$, and SO$_4^{2-}$/Cl$^-$, clearly demonstrates the presence of seawater influence within the coastal aquifers of the study area.

Keywords Groundwater · Seawater intrusion · Major ionic changes · Ionic ratio · HFE-Diagram

P. Moorthy · S. Sundaramoorthy · L. Chokklingam (✉)
Centre for Disaster Management and Coastal Research,
Department of Remote Sensing, Bharathidasan University,
Tiruchirappalli, Tamil Nadu 620 023, India
e-mail: drlaks@bdu.ac.in

P. D. Roy
Instituto de Geología, Universidad Nacional
Autónoma de México (UNAM), Ciudad Universitaria,
04510 Mexico City, CP, Mexico

T. Usha · S. K. Dash
National Centre for Coastal Research, Ministry of Earth
Sciences, Government of India, Chennai 600100, India

M. Gowrappan
French Institute of Pondicherry, Puducherry 605001, India

Introduction

Coasts, where land meets the sea, are densely populated regions with extensive development worldwide. Most of the world's largest cities are situated near rivers or coastlines (Post, 2005). However, river water alone cannot satisfy the ever-increasing water demands of these coastal cities. In these coastal areas, groundwater plays a crucial role as a source of water supply, and coastal aquifers, which hold groundwater, are often considered pristine (Mondal et al., 2010a). However, the purity of these aquifers is constantly challenged by the degradation of groundwater quality linked to the growth of populations and industrialization. The primary issue affecting coastal groundwater quality is salinization which is influenced by various factors such as seawater intrusion, interactions between rocks and water, excessive exploitation, rising sea levels, climatic changes, the hydrogeological characteristics of the study area, salt production, improper sewage disposal, excessive use of chemical fertilizers and pesticides, and marine geological formations (Peters and Meyberck, 2000; Zhang et al., 2011; Fatoric and Chelleri, 2012; Periyasamy et al., 2021). Among these factors, seawater intrusion is recognized as a significant global threat to coastal aquifers (Somay and Gemici, 2009; Cobaner et al., 2012; Batayneh et al., 2014; Anders et al., 2014). It is crucial to recognize as the seawater intrusion is a constantly changing process and these changes can be elucidated by analysing the changes in groundwater chemistry (Richter and Kreitler, 1993; Somay and Gemici, 2009). Therefore, assessing the hydrochemical characteristics of the groundwater can prove valuable in comprehending the movement of seawater intrusion (Sarwade et al., 2007; Ravikumar and Somashekar, 2013; Al-Taani, 2013). The interactions among groundwater and seawater within coastal aquifers are influenced by a multitude of factors. These include sea level elevation, the geological and hydrogeological characteristics of the coastline, cyclones and storm surges, tidal dynamics, reductions in river navigability, and variations in pumping rates from freshwater and groundwater wells (Todd & Mays, 2004; Longe et al., 1987; Saxena et al., 2003; Pulido-Laboeuf, 2004; Lee & Song, 2007; Kouzana et al., 2009; Mondal et al., 2010b; Ayolabi et al., 2013).

Researchers from around the world have conducted numerous studies aimed at identifying and quantifying the intrusion of seawater into coastal aquifers (Sivan et al., 2005; Khublaryan et al., 2008). There exist several methods that can be employed to investigate the salinization of groundwater, such as the hydrochemical facies evolution method (HFE-D) (Giménez-Forcada, 2014) and the freshwater-seawater interaction approach (Mondal et al., 2010a and 2010b). The hydrochemical features and salt content in the groundwater of the study area revealed distinct pollution sources. The primary factor was pinpointed as saline groundwater locations, the second factor indicated sources from agricultural and urban activities, and the third factor identified weathering sources from the geological formations in the study area, unaffected by seasonal variations (Gopinath, et al., 2018). The spatial distribution of groundwater quality in coastal region of Nagapattinam District derived using the water quality index revealed unfit for drinking and is suitable for domestic usage and agriculture with effective crop management practices (Kuttimani et al., 2017). The objective of this study is to assess fluctuations in hydrochemistry and explore the interactions between groundwater and seawater in the coastal aquifers of Nagapattinam, Tamil Nadu. This study involves analysing groundwater chemistry, examining major ion changes, creating ionic ratio plots, investigating hydrochemical facies evolution (HFE-D), and mapping the extent of seawater intrusion. Through these analyses, the study aims to provide a novel and comprehensive understanding of the hydrochemical dynamics in the study area, specifically focusing on the impact of seawater intrusion on groundwater quality and its spatial distribution, in contrast to studies that primarily concerned on water quality indices, drinking suitability, and prediction modeling. The results of this analysis are quantified and spatial-temporal variation in the extent of seawater intrusion was mapped through the use of a Geographical Information System (GIS).

Study area

The study area includes the districts of Nagapattinam, Mayiladuthurai, and Karaikal, situated in the southeastern coastal region of Tamil Nadu, India. It lies between latitudes 10°15′N to 11°30′N and longitudes 79°30′E to 79°55′E with an average elevation of 20 m above mean sea level. The study area

covers approximately 1316 km^2 and has a population density ranging from 400 to 800 persons/km^2. The temperature ranges between 19.3 and 40.6 °C, with relative humidity fluctuating between 70 and 77%, peaking during October to November. The region features diverse soil types including clayey, periodically flooded land, sandy, and loamy soil. This coastal zone presents a unique blend of geographical features, hydrogeological conditions, major river systems, and climatic characteristics. The climate in these districts is tropical, influenced by both the northeast and southwest monsoons. The region experiences distinct wet and dry seasons, with the northeast monsoon (October to December) contributing a significant portion of the annual rainfall. The average annual precipitation accounts about 1230 mm. The major River Cauvery is the primary drainage system in the study area. Its tributaries—Nandhalar, Uppanar, Arasalar, Nattar, and Thirumullairajan—drain the region. Minor irrigation channels criss-cross the deltaic region (Fig. 1).

Geology and hydrogeology

The principal aquifer system consists of coastal alluvium along the coast and fluvial alluvium in the interior, varying in their characteristics and depth. The aquifer characteristics within the study area show a range of transmissivity from 8 to 1672 m^2/day, with storativity of about 4.40×10^{-10} (CGWB, 2008). These aquifers play a crucial role in supporting groundwater resources that are essential for irrigation, domestic use, and industrial activities. The study area's groundwater is found in semi-confined and confined aquifers, including alluvial deposits, sandstone, limestone, and metamorphic rocks. Marine sediments, with their high permeability and proximity to the sea, make coastal aquifers susceptible to seawater intrusion by allowing easy movement of water and creating a shorter pathway for rapid seawater intrusion (Fig. 1). The lower Miocene and Pliocene-Quaternary shallow aquifers play crucial roles, with specific capacity ranging from 13.43 to 870 l per minute per metre of drawdown, and transmissivity from 11 to 1202 m^2/day. Groundwater extraction occurs through various wells. The geology is characterized by sedimentary formations dating back to the Miocene and Quaternary periods. Alluvium, sandstones,

clay marls, siltstones, and clays make up the Quaternary formations. Pliocene deposits known as Karaikal beds include sands, clay, and minor limestone.

Materials and methods

Groundwater sampling techniques

Groundwater samples were collected from two distinct sampling seasons conducted in premonsoon 2020 (PRM 2020) and postmonsoon 2021 (POM 2021). Groundwater within this region was primarily pumped for purposes of drinking, domestic water supply, and irrigation. Field measurements included pH, electrical conductivity (EC), total dissolved solids (TDS), salinity, and temperature were measured in field using a pocket-sized PCSTestr35 probe. Samples were collected in plastic bottles with a capacity of 1 l, which had been previously treated with acid to eliminate impurities. Subsequently, these bottles were sealed and preserved at a temperature of 4 °C after sampling (Clesceri et al., 1989; Kazi et al., 2009). The analysis of major ions (Na^+, Ca^{2+}, Mg^{2+}, K^+, CO_3^{2-}, HCO_3^-, Cl^-, and SO_4^{2-}) was carried out in accordance with the established procedures (APHA, 1998). The concentration levels of calcium (Ca^{2+}) and magnesium (Mg^{2+}) were assessed through the EDTA titration method. Bicarbonate (HCO_3^-) concentration was estimated by volumetric titration (hydrochloric acid method). The determination of chloride (Cl^-) concentrations was carried out using argentometric titration. For the analysis of sulphate (SO_4^{2-}) concentrations, UV-visible spectrophotometry was employed. Sodium (Na^+) and potassium (K^+) concentrations were determined using a flame photometer. Ion balance error (IBE) calculation, based on milliequivalent ions per litre (meq/l), serves as an indicator of the analytical precision, ensuring that it falls within the standard tolerance of $\pm10\%$. The statistical description of major ion concentration in meq/l is shown in Table 1.

Hydrochemical facies evolution

The hydrochemical facies evolution diagram (HFE-Diagram) is a complex graphical representation used for the analysis of seawater intrusion. It serves as a valuable tool for assessing the condition of a
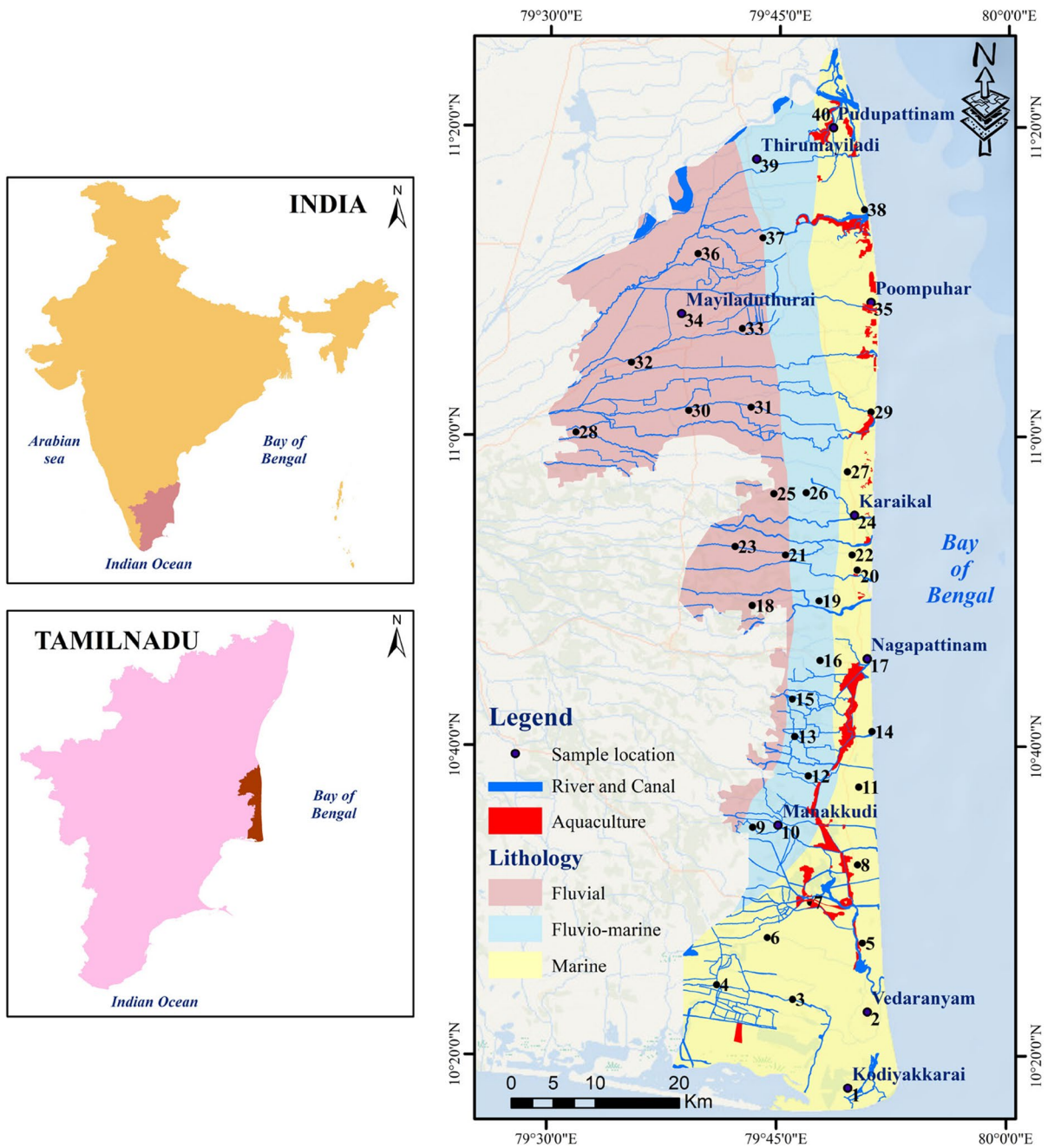
Fig. 1 Location map of groundwater samples during premonsoon 2020 and postmonsoon 2021 from Nagapattinam, Mayiladuthurai, and Karaikal districts, Southeast coast of India

coastal aquifer concerning both intrusion and freshening phases. The HFE-Diagram identifies four heteropic facies: Na-Cl (seawater); Ca-HCO$_3$ (natural fresh water); Ca-Cl (salinized water with reverse exchange); and Na-HCO$_3$ (salinized water with direct exchange). The two primary phases include as follows: freshening (FW) and intrusion (SW) (Giménez-Forcada, 2014). As seawater infiltrates the aquifer, the water undergoes a transformation from a Ca-HCO$_3$ composition to a Na-Cl composition, passing through

Table 1 Statistical description of range of hydrochemical parameters analysed in groundwater samples collected during premonsoon 2020 and postmonsoon 2021 from Nagapattinam, Mayiladuthurai, and Karaikal districts, Southeast coast of India

Season		pH	EC	Ca^{2+}	Mg^{2+}	Na^+	K^+	HCO_3^-	SO_4^{2-}	Cl^-
		-	µS/cm	meq/l	meq/l	meq/l	meq/l	meq/l	meq/l	meq/l
Premonsoon 2020	Min	7.2	424	1.7	0.2	0.96	0.62	0.3	0.61	1.21
	Max	9.35	6990	23.3	4.8	82.95	18.68	5.4	5.60	47.14
	Avg	8.33	1673.2	5.22	1.90	17.05	5.24	2.03	1.80	7.06
	St. dev.	0.54	1359	3.92	0.82	16.25	4.64	1.21	0.92	9.42
Postmonsoon 2021	Min	6.89	368	1.5	0.6	0.6	0.53	0.9	0.20	1.21
	Max	8.62	7010	26.3	5.2	101.38	34.10	8.9	5	51.85
	Avg	7.69	1716.8	7.05	2.30	18.25	6.84	3.79	1.73	8.43
	St. dev.	0.43	1354.3	5.62	1.11	20.91	6.71	2.15	1.06	10.19

an intermediate Ca-Cl composition that is distinctive to the process. This hydrochemical facies is associated with reverse cation exchange reactions influenced by the sodic water as shown in the equation below (Appelo and Geirnaert, 1983).

$$Na^+ + Ca - [clay] = Ca^2 + + [clay] - Na \qquad (1)$$
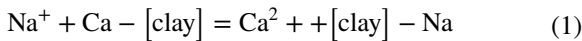
In the freshening phase, the Na-Cl facies undergoes a gradual transition to Ca-HCO₃ facies. However, this transition takes place through an intermediate Na-HCO₃ facies. The distinct feature of the freshening phase is clarified by the direct exchange reactions that contribute to the rise of Na^+ in the water through the following equation (Appelo and Geirnaert, 1983).

$$Ca^{2+} + Na - [clay] = Na^+ + [clay] - Ca \qquad (2)$$
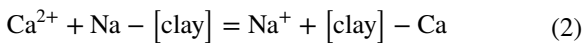
This diagram is divided into two sections by the conservative mixing line (CML). Water samples situated above and to the left of the CML represent the freshening phase, whereas water samples positioned below and to the right of the CML represent the intrusion phase.

The freshening and intrusion fields of the HFE-Diagram have been divided into sub-stages. The freshening sub-stages are designated as f_1, f_2, f_3, f_4, and FW, while the intrusion sub-stages are designated as i_1, i_2, i_3, i_4, and SW. The f_1 sub-stage (Mix Na–Cl facies) is the initial stage of freshening, where the groundwater is still relatively saline. The f_2 sub-stage (Mix Na–Mix Cl facies) is the middle stage of freshening, where the groundwater is becoming less saline. The f_3 sub-stage (Mix Ca–Mix HCO₃ and

Ca–Mix HCO₃ facies) is the late stage of freshening, where the groundwater is almost indistinguishable from freshwater. The f_4 sub-stage (Ca-HCO₃ facies) is the final stage of freshening, where the groundwater is freshwater. The i_1 sub-stage (Ca–MixHCO₃ facies) is the initial stage of intrusion, where the groundwater is still relatively fresh. The i_2 sub-stage (MixCa–Mix Cl, Ca–Mix Cl facies) is the middle stage of intrusion, where the groundwater is becoming more saline. The i_3 sub-stage (Mix Na–Cl, Mix Ca–Cl, Ca–Cl facies) is the late stage of intrusion, where the groundwater is almost indistinguishable from seawater. The i_4 sub-stage (Mix Na–Cl facies) is the final stage of intrusion, where the groundwater is seawater. The SW and FW sub-stage refers to seawater and freshwater, respectively. The different sub-stages of the freshening and intrusion fields in the HFE-Diagram are quantified by assigning them values from 1 to 10, with 1 being the lowest value for freshwater and 10 being the highest value for saline water. The freshening sub-stages are characterized by groundwater with values from 2 to 5, while the intrusion sub-stages are characterized by groundwater with values from 6 to 9. The value 5.5 indicates the point at which the groundwater is transitioning from the freshening phase to the intrusion phase.

Results and discussion

Ionic ratio plots

In the present study, we calculated ionic ratios such as HCO_3^-/Cl^-, Ca^{2+}/Na^+, Na^+/Cl^-, Ca^{2+}/Cl^-, $Mg^{2+}/$

Cl^-, K^+/Cl^-, SO_4^{2-}/Cl^-, Na^++K^+, and $Ca^{2+}+Mg^{2+}$ and plotted against TDS. The bivariate plot between Cl vs TDS shows a strong linear correlation irrespective of monsoon ($r^2 = 0.95$ in PRM 2020 and $r^2=0.89$ in POM 2021). In both PRM 2020 and POM 2021, the ratio of HCO_3^-/Cl^- in all the groundwater samples analysed was greater than seawater ratio 0.0069 and this ratio gradually decreases and gets close to the seawater ratio (Fig. 2a). This suggests more seawater is getting intruded into the coastal aquifers and the ratio can be a good sign of water becoming salty because of seawater intrusion. Ca^{2+}/Na^+ vs TDS plot indicates that high TDS is associated with high Cl^- and Na^+ concentration. Therefore, it shows negative relationship with TDS, whereas Na^+/Ca^{2+} vs TDS indicates good relationship between each other which is indicative of cation exchange reaction (Edet & Okereke, 2002). This indicates that high Cl^- and Na^+ significantly contribute to the increase in TDS, making it a valuable tool for studying seawater intrusion (Saxena et al., 2003; Batayneh et al., 2014; Nwankwoala and Udom, 2011) (Fig. 2b, c). The Na^+/Cl^- ratio does not exhibit any correlation with TDS, suggesting the coexistence of both ions during the intrusion phase of both monsoons (Batayneh et al., 2014). The Na^+/Cl^- ratio ranges from 0.26 to 13.97 and from 0.33 to 5.48 with an average of 3.10 and 2.26 during PRM 2020 and POM 2021, respectively. At about, 18 (7 samples) and 10% (4 samples) showed low Na^+/Cl^- ratio (<1) due to seawater intrusion as they were located near to the coast during PRM 2020 and POM 2021, respectively. The remaining 82 (33 samples) in PRM 2020 and 90% (36 samples) in POM 2021 showed high Na^+/Cl^- ratio (>1) due to anthropogenic influence in to groundwater (Wang and Jiao, 2012; Krishnakumar et al., 2014; Shi et al., 2018) (Fig. 2d).

Apart from these, other ionic ratios such as Ca^{2+}/Cl^-, Mg^{2+}/Cl^-, K^+/Cl^-, and SO_4^{2-}/Cl^- show a negative trend in both the monsoon, indicating an increase in chloride concentration and subsequently higher TDS levels with a decrease in these ratios (Fig. 2e, f, g, and h). The Na^++K^+ ratio vs TDS plot reveals a strong positive correlation ($r^2=0.78$) during the postmonsoon (POM 2021), in contrast to the premonsoon (PRM 2020) which shows moderate correlation ($r^2=0.53$). This suggests a distinct signature of groundwater salinization between the monsoons (Fig. 2i). Likewise, plot $Ca^{2+}+Mg^{2+}$ vs. TDS in the postmonsoon period exhibits a strong correlation ($r^2=0.73$), while in the premonsoon period, it shows moderate correlation ($r^2=0.59$). Thus, the phenomenon could be attributed to the recharging of groundwater during the postmonsoon season, which leads to the freshening of groundwater (Fig. 2j).

Hydrochemical facies evolution for identifying seawater intrusion process

In PRM 2020, about 65 and 35% of samples falls under freshening and intrusion phase, respectively. About seven and four hydrochemical facies were identified in freshening and intrusion phase of HFE-Diagram, respectively. The seven facies of freshening phase include Na-Cl, Na-MixCl, MixNa-MixCl, Na-MixHCO$_3$/MixSO$_4$, MixNa-MixSO$_4$, Na-HCO$_3$, and MixCa-HCO$_3$. The four facies of intrusion phase include MixCa-MixHCO$_3$, MixNa-Cl, Ca-Cl, and Na-Cl. Among these facies, the largest percentage (30%) is contributed by Na-Cl (f_1) facies of freshening phase (Table 2) (Fig. 3a). In POM 2021, about 72.5 and 27.5% of samples were categorized under freshening and intrusion phase, respectively. About five and three hydrochemical facies were identified in freshening and intrusion phase respectively. The five facies of freshening phase include Na-Cl, Na-MixCl, Na-MixHCO$_3$/MixSO$_4$, MixNa-MixSO$_4$, and Na-HCO$_3$. The three facies of intrusion phase include MixNa-Cl, Na-Cl, and MixCa-Cl. Similar to PRM 2020, Na-Cl facies of freshening facies (f_1) continued to be predominant with largest percentage of 30% (Table 2) (Fig. 3b).

In PRM 2020, impact of salinization due to intrusion phase is observed along the south, southeastern, and as patches in northeastern part of the study area, near to Bay of Bengal. Patches of freshening facies from f_1 to f_4+Freshwater via f_2 and f_3 facies were observed along east-west direction in the northwestern part of the study area, indicating the less impact of salinization. In POM 2021, a significant regression of seawater occurs as a result of precipitation and recharge, particularly in the southeastern and northeastern part of the study area (Ahmad et al., 2003; Ray & Mukherjee, 2008). However, at close proximity to the sample no.7 in southern part, the study area experiences continuous salinization impact during both PRM 2020 and POM 2021 due to numerous aquaculture activities (Gopinath et al., 2019). Coastal
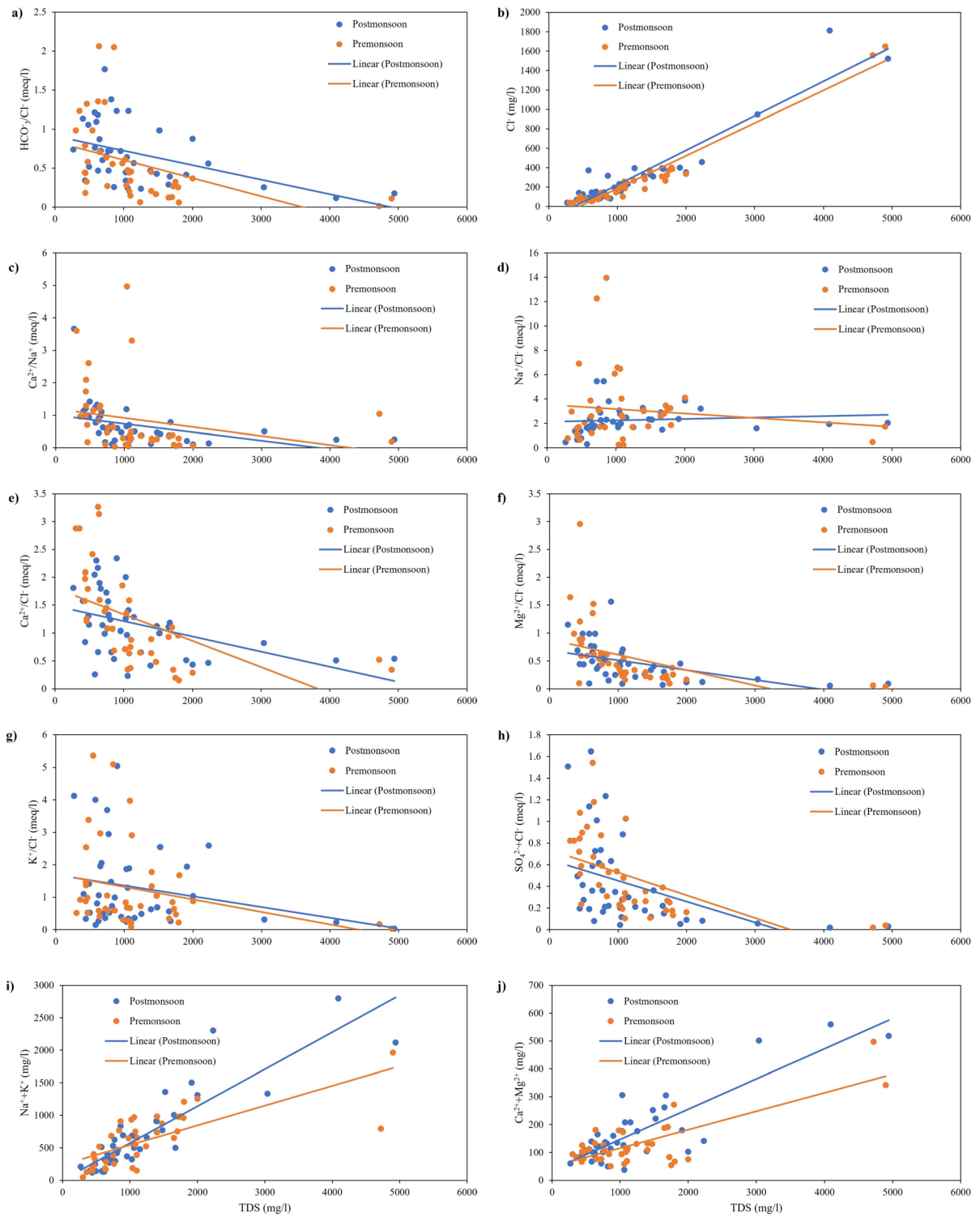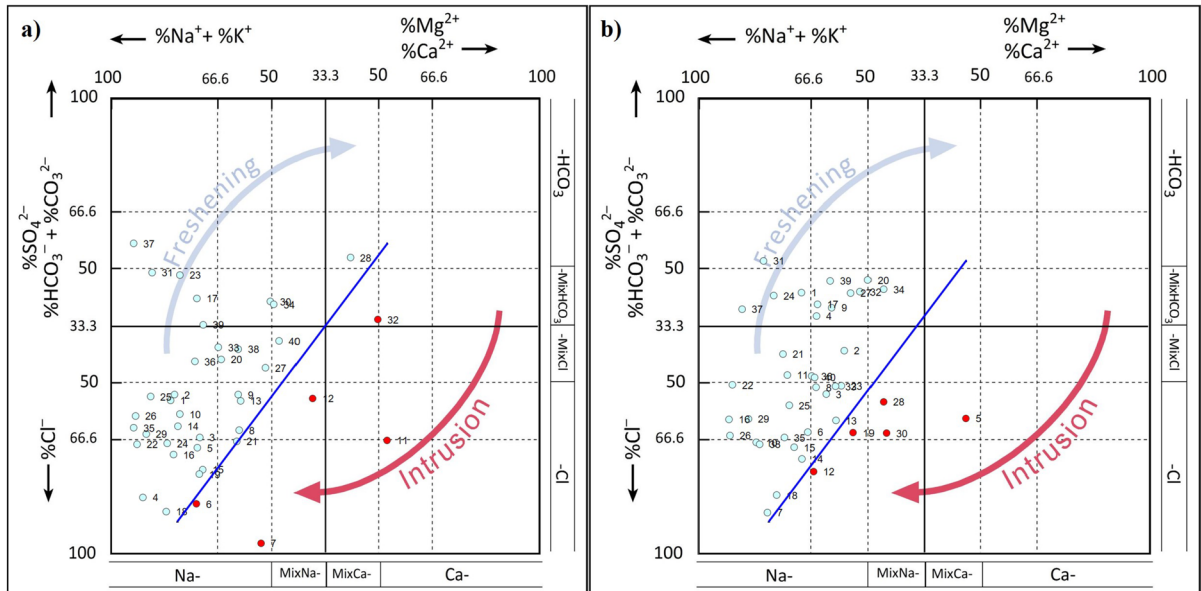
Fig. 2 Ionic ratio plot of TDS vs HCO_3^-/Cl^- (**a**), Cl^- (**b**), Ca^{2+}/Na^+ (**c**), Na^+/Cl^- (**d**), Ca^{2+}/Cl^- (**e**), Mg^{2+}/Cl^- (**f**), K^+/Cl^- (**g**), SO_4^{2-}/Cl^- (**h**), Na^++K^+ (**i**), and $Ca^{2+}+Mg^{2+}$ (**j**) for groundwater samples collected during premonsoon 2020 and postmonsoon 2021 from Nagapattinam, Mayiladuthurai, and Karaikal districts, Southeast coast of India

Table 2 Illustration of hydrochemical facies of groundwater samples collected during premonsoon 2020 and postmonsoon 2021 from Nagapattinam, Mayiladuthurai, and Karaikal districts, Southeast coast of India

Hydrochemical facies	Sub-stage	Facies	No. of samples	% of samples	Overall %
Premonsoon 2020					
Freshening	f_1	Na-Cl	12	30	65
	f_2	Na-MixCl	5	12.5	
	f_2	MixNa-MixCl	1	2.5	
	f_3	Na-MixHCO$_3$/MixSO4	5	12.5	
	f_3	MixNa-MixSO4	1	2.5	
	f_4 + freshwater	Na-HCO3	1	2.5	
	f_4 + freshwater	MixCa-HCO$_3$	1	2.5	
Intrusion	i_1	MixCa-MixHCO$_3$	1	2.5	35
	i_3	MixNa-Cl	1	2.5	
	i_4 + seawater	Ca-Cl	1	2.5	
	i_4 + seawater	Na-Cl	11	27.5	
Postmonsoon 2021					
Freshening	f_1	Na-Cl	12	30	72.5
	f_2	Na-MixCl	5	12.5	
	f_3	Na-MixHCO$_3$/MixSO$_4$	10	25	
	f_3	MixNa-MixSO$_4$	1	2.5	
	f_4 + freshwater	Na-HCO3	1	2.5	
	i_3	MixNa-Cl	2	5	27.5
	i_3	Na-Cl	1	2.5	
	i_3	MixCa-Cl	1	2.5	
	i_4 + seawater	Na-Cl	7	17.5	

Fig. 3 Hydrochemical facies evolution-diagram (HFE-D) showing freshening and intrusion phases of groundwater samples collected during premonsoon 2020 (**a**) and postmonsoon 2021 (**b**) from Nagapattinam, Mayiladuthurai, and Karaikal districts, Southeast coast of India

regions with permeable soils and porous rock formations, urbanization, land reclamation, reduced freshwater discharge into coastal aquifers, unregulated aquaculture, and saltpan practices are major factors for intrusion along the coastal areas, while inland salinization is due to excessive pumping of groundwater from wells for agricultural, industrial, and domestic purposes, improper irrigational practices using excessive fertilizers.

The occurrences of freshening and intrusion phases during PRM 2020 and POM 2021 were represented through heatmaps generated using Arc-GIS software. Spatial distribution maps were created using the spline method in ArcView spatial analyst tool to visualize the differences of these phases (Figs. 4 and 5). This method interpolates the data across a continuous surface based on a set of sample points that passes through the input points while minimizing overall curvature (Giménez-Forcada, 2014). The

heatmaps show that the aquifer is experiencing nearly constant salinization, with its boundary situated on the southern and eastern part of the study area, close to Bay of Bengal, where it is influenced by seawater intrusion. The process of freshening is situated in northwestern part of the study area during both PRM 2020 and POM 2021.

Major ionic changes

Ionic changes during seawater–groundwater mixing refer to the alterations in the concentration of dissolved ions. When seawater and groundwater come into contact and mix, it leads to various changes in the chemical composition. These chemical reactions can be understood by comparing the theoretical mixing values of freshwater and seawater with the ion concentrations of collected groundwater samples. By considering the fact that Cl^- is a conservative

Fig. 4 Heatmap showing spatial distribution of hydrochemical facies of groundwater samples collected during premonsoon 2020 from Nagapattinam, Mayiladuthurai, and Karaikal districts, Southeast coast of India
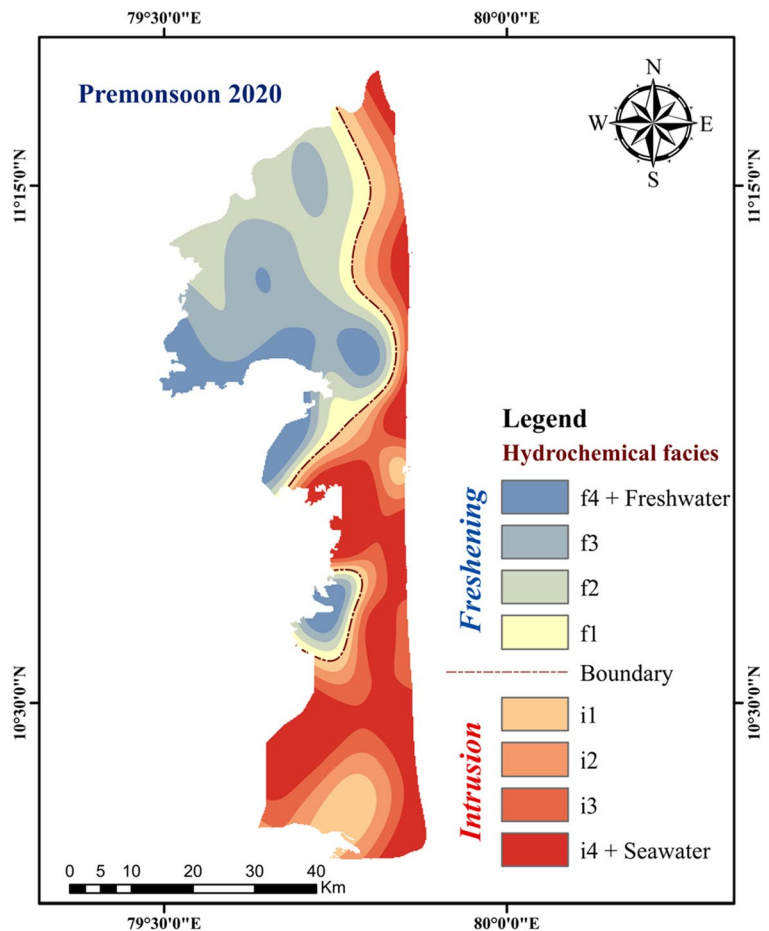
Fig. 5 Heatmap showing spatial distribution of hydrochemical facies of groundwater samples collected during postmonsoon 2021 from Nagapattinam, Mayiladuthurai, and Karaikal districts, Southeast coast of India
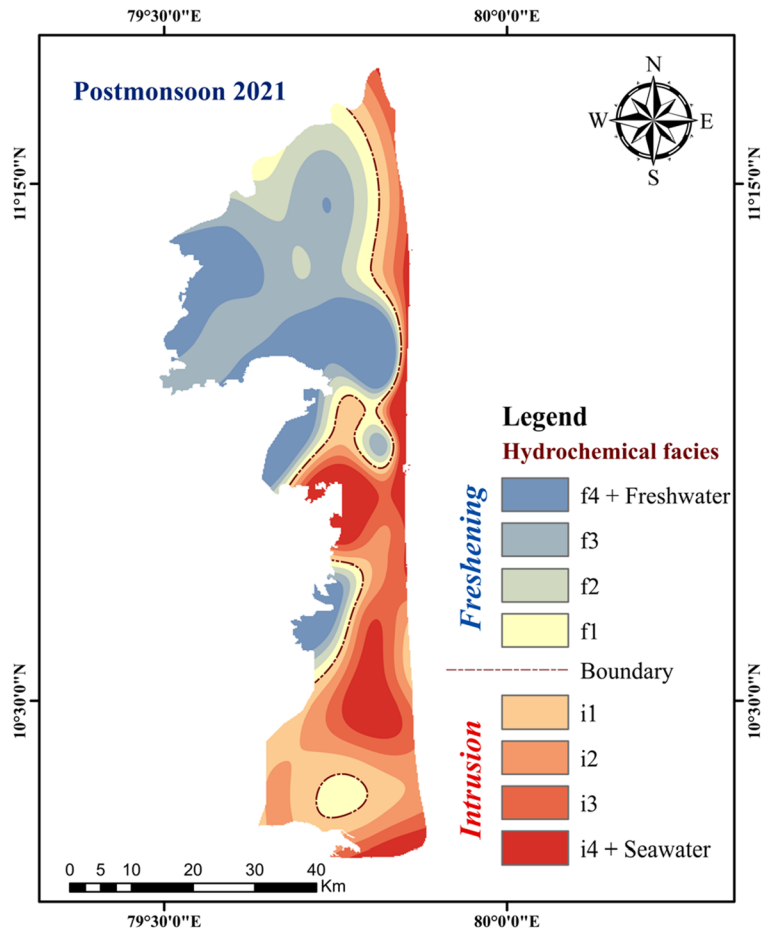

element, seawater fraction in samples was calculated (Svensson et al., 2012). The seawater fraction in each sample was used to assess the changes in the ionic composition of Na^+, Ca^{2+}, Mg^{2+}, K^+, HCO_3^-, and SO_4^{2-} that took place during the interaction (Table 3). About, 50% (20 samples) showed positive

seawater fraction (f_{sea}) and indicated the mixing process between seawater and freshwater, irrespective of season (Mondal et al., 2010a and 2010b).

Calculated ionic changes of ions such as Na^+, Ca^{2+}, Mg^{2+}, K^+, HCO_3^-, and SO_4^{2-} during PRM 2020 and POM 2021 are represented in Fig. 6.

Table 3 Representation of major ionic changes groundwater samples collected during premonsoon 2020 and postmonsoon 2021 from Nagapattinam, Mayiladuthurai, and Karaikal districts, Southeast coast of India

Ions	Seawater (meq/l)	Freshwater (meq/l)	Premonsoon 2020 Ionic changes (meq/l)		Postmonsoon 2021 Ionic changes (meq/l)	
			Min	Max	Min	Max
Ca^{2+}	21.05	3.04	−1.59	18.69	−1.61	21.40
Mg^{2+}	32.3	0.99	−2.06	4.03	−1.42	3.75
Na^+	1126	0.04	−75.95	42.16	−14.73	26.18
K^+	10.96	0.12	0.36	18.41	0.26	33.78
HCO_3^-	1.49	5.83	−5.56	−0.10	−4.96	3.12
SO_4^{2-}	45.8	0.83	−3.95	4.71	−4.53	4.09
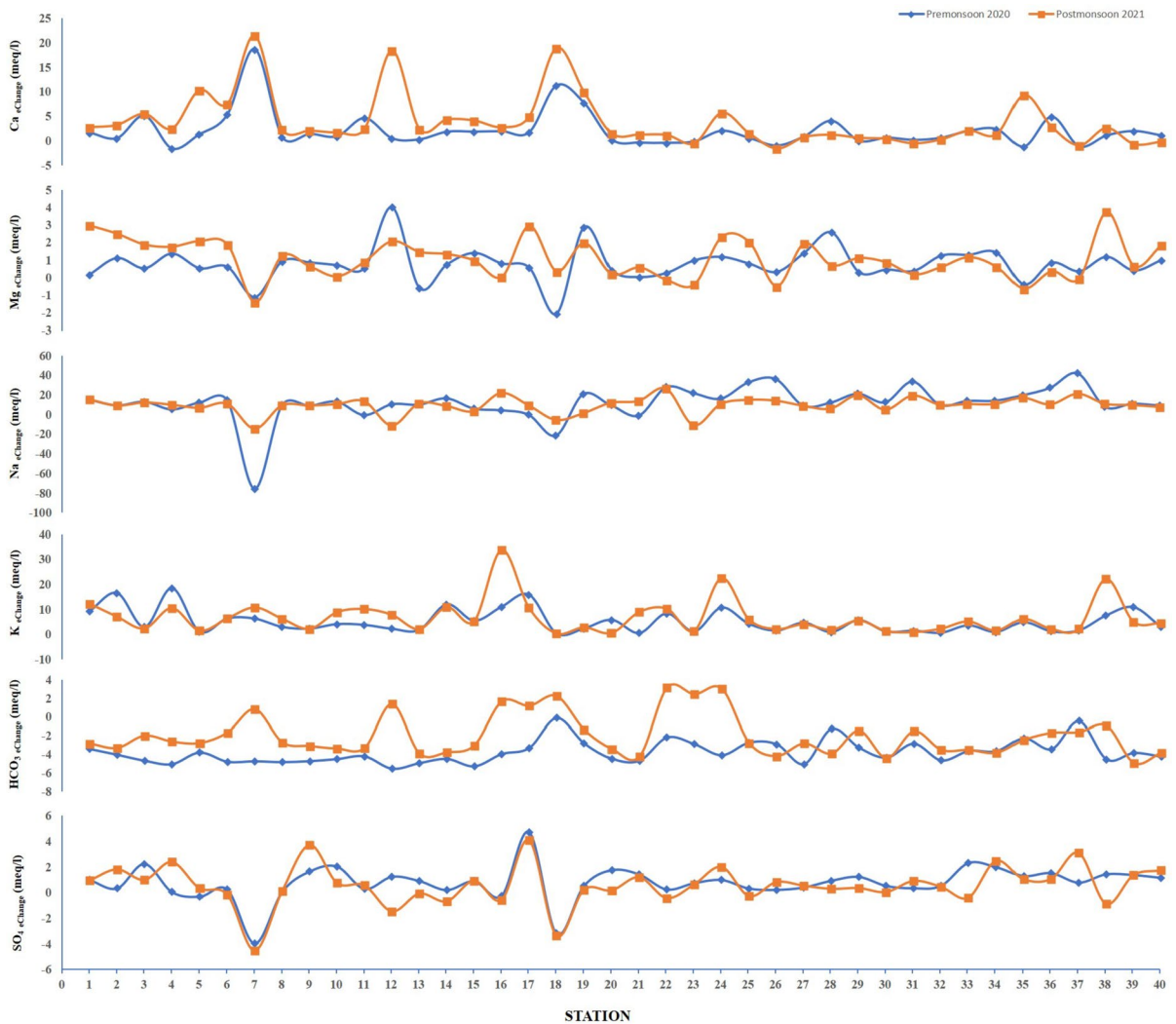
Fig. 6 Major ionic changes of groundwater samples collected during premonsoon 2020 and postmonsoon 2021 from Nagapattinam, Mayiladuthurai, and Karaikal districts, Southeast coast of India

Among all ions, Na^+ and Ca^{2+} showed unique ionic change pattern, due to mixing process of seawater with groundwater. Since Na^+ concentration in freshwater is less, $Na_{echange}$ in fresh groundwater showed positive and groundwater samples intruded with seawater showed negative trend. In the present study, ionic $Na_{echange}$ ranged between -75.95 and 42.16 meq/l with an average of 11.48 meq/l during PRM 2020 and between -14.73 and 26.18 meq/l with an average of 9.29 meq/l during POM 2021. In contrast, Ca^{2+} concentration in freshwater is more and $Ca_{echange}$ value is negative for fresh groundwater and positive for groundwater mixed with seawater. The

ionic $Ca_{echange}$ ranged from -1.59 to 18.69 meq/l with an average of 2.09 meq/l and from -1.61 to 21.40 meq/l with average of 3.87 meq/l during PRM 2020 and POM 2021 respectively. The negative $Ca_{echange}$ values were observed in groundwater samples located far away the coast is due to carbonate dissolution (Mondal et al., 2011).

In general, chemical composition of the natural groundwater in the coastal region will be primarily characterized by high concentrations of Ca^{2+} and HCO_3^-, due to the dissolution of carbonates (Mondal et al., in 2011). The dominant ions present in seawater consist of Na^+ and Cl^- and their presence indicated

the seawater intrusion in the coastal aquifers of the study area (Appelo and Postma, 2005). However, the seawater intrusion can be explained more by cation exchange between Na^+ and Ca^{2+} - Mg^{2+} (Pulido-Laboeuf, 2004). Also, the negative $K^+_{echange}$, positive $Mg^{2+}_{echange}$, and positive $SO_4^{2-}_{echange}$ values support the samples that show negative $Na_{echange}$ and positive $Ca_{echange}$ values, indicating seawater intrusion along the coastal aquifers of study area (Aris et al., 2009; Mondal et al., 2010a).

Conclusion

In this study, hydrochemical methodologies have been employed to examine the phenomenon of seawater intrusion within the coastal aquifers of the Nagapattinam, Mayiladuthurai, and Karaikal region, Southeast coast of India. Groundwater samples were collected and subjected to analysis to gain insights into the development of hydrochemical facies and the processes of ion exchange in reaction to seawater intrusion. This study concludes that the aquifer currently experiences widespread salinization and the amount of recharge it receives is inadequate to restore the aquifer's water quality to its previous state before salinization occurred. Since Tamil Nadu gets more rainfall from the northeast monsoons than the southwest monsoon, it has a positive effect on groundwater quality, making it better compared to postmonsoon groundwater quality. As a result, the average concentrations of certain ions are higher in postmonsoon samples. Ionic ratios serve as a valuable method for delineating regions impacted by seawater intrusion. The connection between total dissolved solids (TDS) and various ionic ratios, such as HCO_3^-/Cl^-, Na^+/Cl^-, Ca^{2+}/Cl^-, Mg^{2+}/Cl^-, K^+/Cl^-, and SO_4^{2-}/Cl^-, clearly demonstrates the presence of seawater influence within the coastal aquifers of the study area.

The HFE-Diagram reveals that the specific changes should be understood as fluctuations associated with the movement of groundwater within the aquifer. The HFE-Diagram analysis reveals that, during the premonsoon 2020, 35% of the samples showed signs of groundwater aquifer being intruded by seawater. The major hydrochemical facies include as follows: $MixCaMixHCO_3$, MixNa-Cl, Ca-Cl, and Na-Cl indicate a direct cation exchange process. In contrast, during the postmonsoon 2021, 27.5% of the samples

displayed evidence of seawater intrusion. The dominant hydrochemical facies in this phase, specifically MixNa-Cl, Na-Cl, and MixCa-Cl, suggest a reverse ion exchange process. Successive phases of intrusion and freshening occur in cycles, influenced by both the extraction of groundwater through pumping and the significant lateral recharge entering the aquifer. Collectively, the assertion that employing the HFE-Diagram and analysing hydrochemical facies significantly enhances the comprehension of hydrochemical data within the context of seawater intrusion into coastal aquifers of study area. This approach directly establishes a connection between freshwater-seawater interaction and groundwater quality. An additional benefit of using the HFE-Diagram becomes evident when its results are spatially visualized through heatmaps. These heatmaps serve as an effective tool for finer investigation and more indirect variations in the aquifer's condition regarding seawater intrusion.

Author contribution PM: writing—original draft preparation; SS: writing—original draft preparation; PDR: writing—reviewing and editing; TU: writing—reviewing and editing; SKD: investigation and data curation; MG: conceptualization, writing—reviewing and editing; LC: methodology, supervision, investigation, writing—reviewing and editing.

Data availability The datasets generated and/or analysed during the current study are available from the corresponding author on reasonable request.

Code availability Not applicable

Declarations

Ethical approval The authors confirm that the manuscript has not been submitted to journal for simultaneous consideration and has not been previously published.

Competing interests The authors declare no competing interests.

References

Ahmad, N., Sen, Z., & Ahmad, M. (2003). Ground water quality assessment using multi-rectangular diagrams. *Groundwater, 41*(6), 828–832.

Al-Taani, A. A. (2013). Seasonal variations in water quality of Al-Wehda Dam north of Jordan and water suitability for irrigation in summer. *Arabian Journal of Geosciences, 6*, 1131–1140.

Anders, R., Mendez, G. O., Futa, K., & Danskin, W. R. (2014). A geochemical approach to determine sources and movement of saline groundwater in a coastal aquifer. *Groundwater, 52*(5), 756–768.

APHA. (1998). *Standard methods for the examination of water and waste water* (20th ed.). *American Public Health Association*.

Appelo, C. J., & Geirnaert, W. (1983). Processus accompanying the intrusion of salt water. *Geologia Applicata e Idrogeologia, 18*(2), 19–40.

Appelo, C. A. J., & Postma, D. (2005). *Geochemistry. Groundwater and pollution* (2nd ed., pp. 241–309).

Aris, A. Z., Abdullah, M. H., Kim, K. W., & Praveena, S. M. (2009). Hydrochemical changes in a small tropical island's aquifer: Manukan Island, Sabah, Malaysia. *Environmental Geology, 56*, 1721–1732.

Ayolabi, E. A., Folorunso, A. F., Odukoya, A. M., & Adeniran, A. E. (2013). Mapping saline water intrusion into the coastal aquifer with geophysical and geochemical techniques: The University of Lagos campus case (Nigeria). *SpringerPlus, 2*(1), 1–14.

Batayneh, A., Zaman, H., Zumlot, T., Ghrefat, H., Mogren, S., Nazzal, Y., et al. (2014). Hydrochemical facies and ionic ratios of the coastal groundwater aquifer of Saudi Gulf of Aqaba: Implication for seawater intrusion. *Journal of Coastal Research, 30*(1), 75–87.

Central Ground Water Board (CGWB). (2008). Ground water resources and development prospects in district Groundwater brochure Nagapattinam District Tamil Nadu. *Techn Report*, 1–20.

Clesceri, L. S., Greenberg, A. E., Eaton, A. D., & Franson, M. A. H. (1989). Standard methods for the examination of water and wastewater.

Cobaner, M., Yurtal, R., Dogan, A., & Motz, L. H. (2012). Three dimensional simulation of seawater intrusion in coastal aquifers: A case study in the Goksu Deltaic Plain. *Journal of hydrology, 464*, 262–280.

Edet, A. E., & Okereke, C. S. (2002). Delineation of shallow groundwater aquifers in the coastal plain sands of Calabar area (Southern Nigeria) using surface resistivity and hydrogeological data. *Journal of African Earth Sciences, 35*(3), 433–443.

Fatorić, S., & Chelleri, L. (2012). Vulnerability to the effects of climate change and adaptation: The case of the Spanish Ebro Delta. *Ocean & Coastal Management, 60*, 1–10.

Giménez-Forcada, E. (2014). Space/time development of seawater intrusion: A study case in Vinaroz coastal plain (Eastern Spain) using HFE-Diagram, and spatial distribution of hydrochemical facies. *Journal of Hydrology, 517*, 617–627.

Gopinath, S., Srinivasamoorthy, K., Vasanthavigar, M., Saravanan, K., Prakash, R., Suma, C. S., & Senthilnathan, D. (2018). Hydrochemical characteristics and salinity of groundwater in parts of Nagapattinam district of Tamil Nadu and the Union Territory of Puducherry, India. *Carbonates and Evaporites, 33*, 1–13.

Gopinath, S., Srinivasamoorthy, K., Saravanan, K., Prakash, R., & Karunanidhi, D. (2019). Characterizing groundwater quality and seawater intrusion in coastal aquifers of Nagapattinam and Karaikal, South India using hydrogeochemistry and modeling techniques. *Human and Ecological Risk Assessment: An International Journal, 25*(1-2), 314–334.

Kazi, T. G., Arain, M. B., Jamali, M. K., Jalbani, N., Afridi, H. I., Sarfraz, R. A., et al. (2009). Assessment of water quality of polluted lake using multivariate statistical techniques: A case study. *Ecotoxicology and Environmental Safety, 72*(2), 301–309.

Khublaryan, M., Frolov, A., & Yushmanov, I. (2008). Seawater intrusion into coastal aquifers. *Water Resour, 35*, 274–286.

Kouzana, L., Mammou, A. B., & Felfoul, M. S. (2009). Seawater intrusion and associated processes: Case of the Korba aquifer (Cap-Bon, Tunisia). *Comptes Rendus Geoscience, 341*(1), 21–35.

Krishnakumar, P., Lakshumanan, C., Kishore, V. P., Sundararajan, M., Santhiya, G., & Chidambaram, S. (2014). Assessment of groundwater quality in and around Vedaraniyam, South India. *Environmental earth sciences, 71*, 2211–2225.

Kuttimani, R., Raviraj, A., Pandian, B. J., & Kar, G. (2017). Determination of water quality index in coastal area (Nagapattinam) of Tamil Nadu, .

Lee, J. Y., & Song, S. H. (2007). Evaluation of groundwater quality in coastal areas: Implications for sustainable agriculture. *Environmental Geology, 52*(7), 1231–1242.

Longe, E. O., Malomo, S., & Olorunniwo, M. A. (1987). Hydrogeology of Lagos metropolis. *Journal of African Earth Sciences (1983), 6*(2), 163–174.

Mondal, N. C., Singh, V. P., Singh, V. S., & Saxena, V. K. (2010a). Determining the interaction between groundwater and saline water through groundwater major ions chemistry. *Journal of Hydrology, 388*(1-2), 100–111.

Mondal, N. C., Singh, V. P., Singh, S., & Singh, V. S. (2010b). Hydrochemical characteristic of coastal aquifer from Tuticorin, Tamil Nadu, India. *Environmental monitoring and assessment, 175*, 531–550.

Mondal, N. C., Singh, V. S., Saxena, V. K., & Singh, V. P. (2011). Assessment of seawater impact using major hydrochemical ions: A case study from Sadras, Tamilnadu, India. *Environmental monitoring and assessment, 177*, 315–335.

Nwankwoala, H. O., & Udom, G. J. (2011). Hydrochemical facies and ionic ratios of groundwater in Port Harcourt. *Southern Nigeria. Res J Chem Sci, 1*(3), 87–101.

Periyasamy, R., Roy, P. D., Chokkalingam, L., Natarajan, L., Sundar, S., Moorthy, P., & Gowrappan, M. (2021). Transformation analysis on landuse/land cover changes for two decades between 1999 and 2019 CE with reference to aquaculture—Nagapattinam coast, southeast India. *Journal of the Indian Society of Remote Sensing, 49*, 2831–2845.

Peters, N. E., & Meybeck, M. (2000). Water quality degradation effects on freshwater availability: Impacts of human activities. *Water International, 25*(2), 185–193.

Post, V. E. A. (2005). Fresh and saline groundwater interaction in coastal aquifers: Is our technology ready for the problems ahead? *Hydrogeology Journal, 13*, 120–123.

Pulido-Leboeuf, P. (2004). Seawater intrusion and associated processes in a small coastal complex aquifer (Castell de Ferro, Spain). *Applied geochemistry, 19*(10), 1517–1527.

Ravikumar, P., & Somashekar, R. K. (2013). A geochemical assessment of coastal groundwater quality in the Varahi river basin, Udupi District, Karnataka State, India. *Arabian Journal of Geosciences, 6*, 1855–1870.

Ray, R. K., & Mukherjee, R. (2008). Reproducing the piper trilinear diagram in rectangular coordinates. *Groundwater, 46*(6), 893–896.

Richter, B.C., & Kreitler, W.C. (1993). Geochemical techniques for identifying sources of groundwater salinization. *CRC Press,* . ISBN 1-56670-000-0

Sarwade, D. V., Nandakumar, M. V., Kesari, M. P., Mondal, N. C., Singh, V. S., & Singh, B. (2007). Evaluation of sea water ingress into an Indian atoll. *Environmental Geology, 52*, 1475–1483.

Saxena, V. K., Singh, V. S., Mondal, N. C., & Jain, S. C. (2003). Use of hydrochemical parameters for the identification of fresh groundwater resources, Potharlanka Island, India. *Environmental Geology, 44*, 516–521.

Shi, X., Wang, Y., Jiao, J. J., Zhong, J., Wen, H., & Dong, R. (2018). Assessing major factors affecting shallow groundwater geochemical evolution in a highly urbanized coastal area of Shenzhen City, China. *Journal of Geochemical Exploration, 184*, 17–27.

Sivan, O., Yechieli, Y., Herut, B., & Lazar, B. (2005). Geochemical evolution and timescale of seawater intrusion into the coastal aquifer of Israel. *Geochimica et Cosmochimica Acta, 69*(3), 579–592.

Somay, M. A., & Gemici, Ü. (2009). Assessment of the salinization process at the coastal area with hydrogeochemical tools and geographical information systems (GIS): Selçuk plain, Izmir, Turkey. *Water, Air, and Soil Pollution, 201*, 55–74.

Svensson, T., Lovett, G. M., & Likens, G. E. (2012). Is chloride a conservative ion in forest ecosystems? *Biogeochemistry, 107*, 125–134.

Todd, D. K., & Mays, L. W. (2004). *Groundwater hydrology*. John Wiley & Sons.

Wang, Y., & Jiao, J. J. (2012). Origin of groundwater salinity and hydrogeochemical processes in the confined Quaternary aquifer of the Pearl River Delta, China. *Journal of Hydrology, 438*, 112–124.

Zhang, E., Savenije, H. H., Wu, H., Kong, Y., & Zhu, J. (2011). Analytical solution for salt intrusion in the Yangtze Estuary, China. *Estuarine, Coastal and Shelf Science, 91*(4), 492–501.